



Figures and figure supplements

ZP4 confers structural properties to the zona pellucida essential for embryo development

Ismael Lamas-Toranzo *et al*

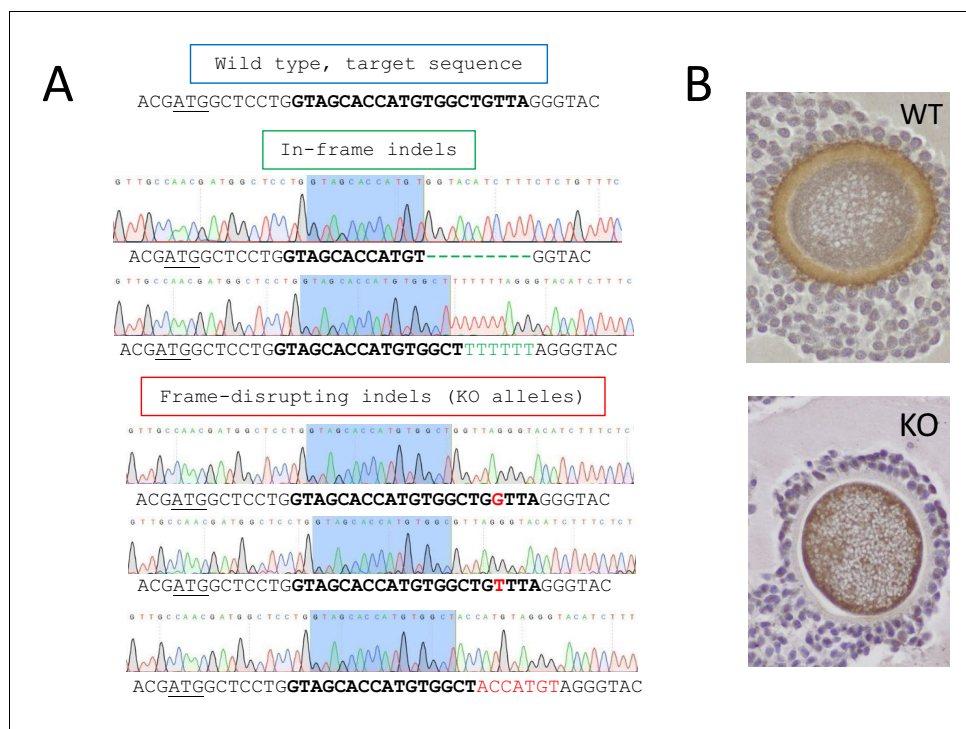
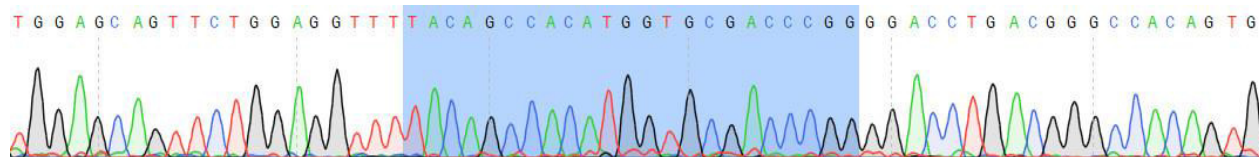


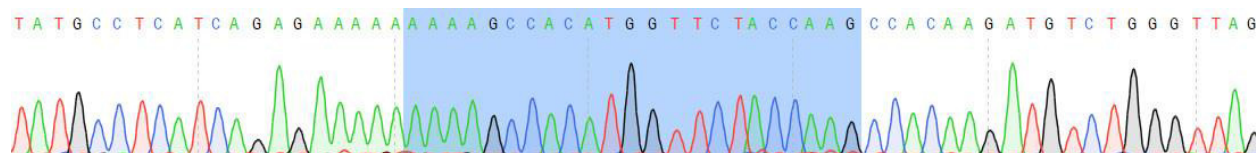
Figure 1. Generation of ZP4 KO rabbits. (A) A sgRNA was designed for a genomic target located at the beginning of the coding region. Upper sequence depicts wild-type sequence with the start codon underlined and CRISPR target sequence marked in bold letters. Examples of different indels obtained in F0 generation are depicted below. Both in-frame indels (i.e., multiple of three) and frame-disrupting (i.e., not multiple of three) were obtained. Only frame disrupting indels generate truly KO alleles by disrupting the ORF of ZP4. The KO allele involving a G insertion was selected to establish a line. (B) Wild-type and ZP4-null cumulus oocyte complexes following immunohistochemistry with an anti-ZP4 antibody.

DOI: <https://doi.org/10.7554/eLife.48904.003>

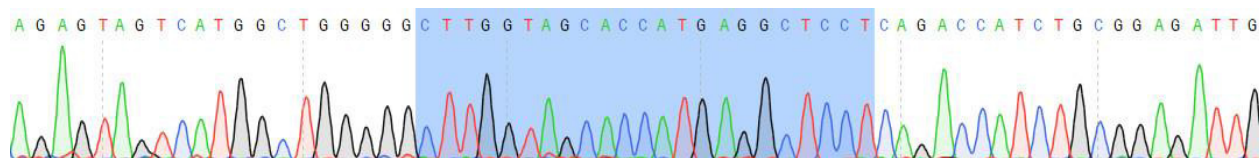
Possible off-target #1: NW_003159362.1 167986-168008; Score: 5.889



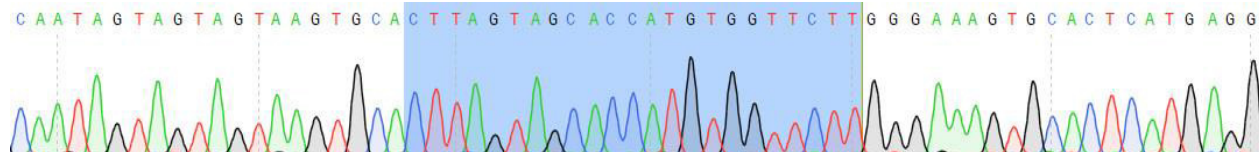
Possible off-target #2: NC_013699.1 57703487-57703465; Score: 2.671



Possible off-target #3: NW_003159579.1 242216-242194; Score: 2.508



Possible off-target #4: NC_013678.1 41151735-41151757; Score: 1.423



Possible off-target #5: NC_013686.1 11746835-11746813; Score: 1.33

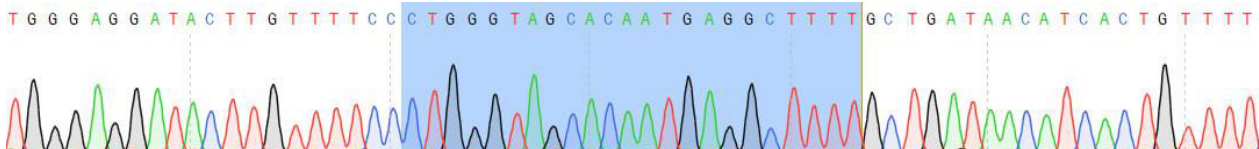


Figure 1—figure supplement 1. Sequencing of the five most probable off-target sequences, revealing no off-target genome editing.

DOI: <https://doi.org/10.7554/eLife.48904.004>

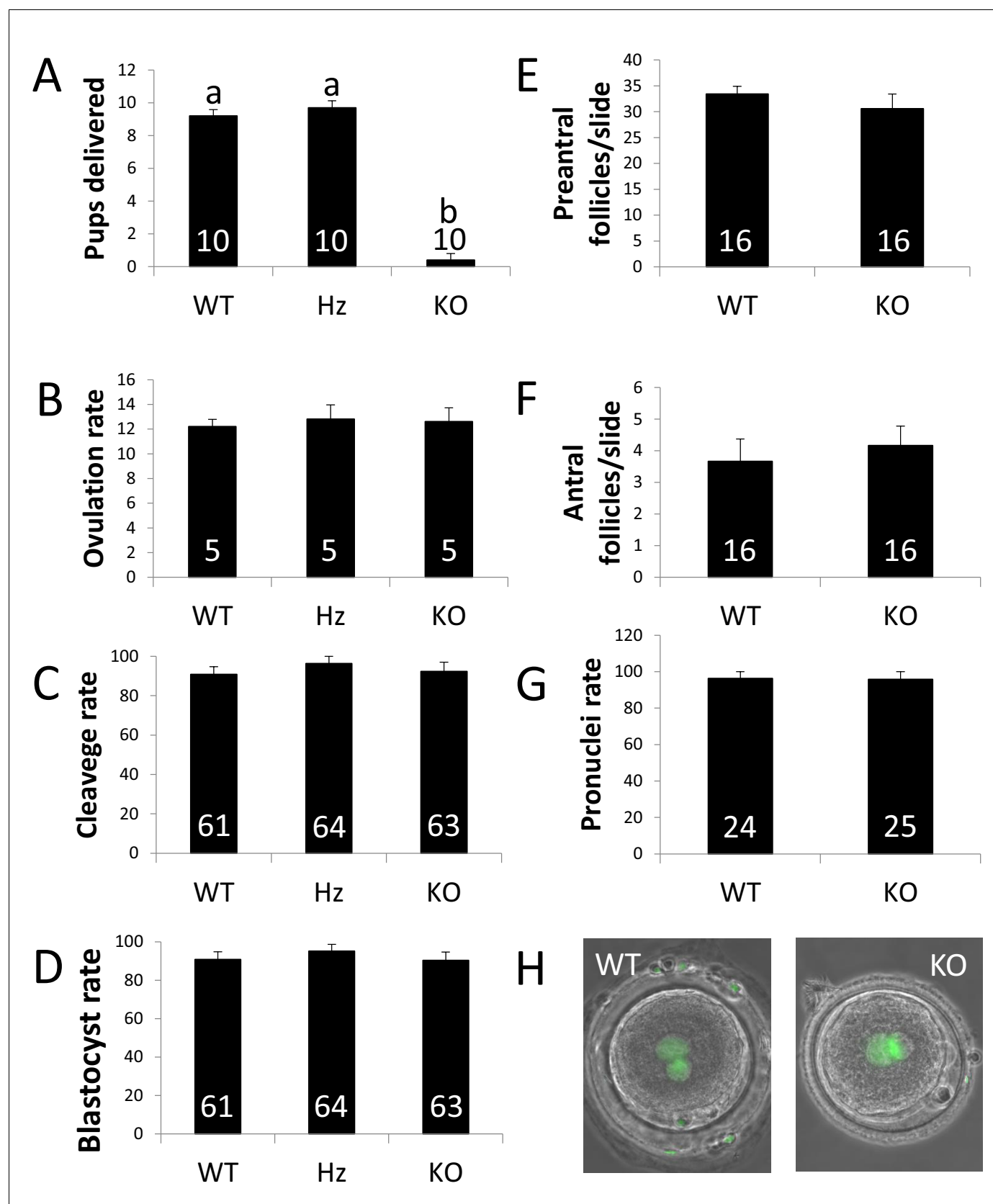


Figure 2. ZP4 ablation leads to severely impaired fertility. (A) Number of pups delivered in WT, Hz and KO females. ZP4 ablation significantly impaired fertility: only one female out of 10 delivered a small litter of 4 pups, whereas ZP4 haploinsufficiency (Hz) did not affect fertility. (B–G) ZP4 disruption did not affect fertility. (H) ZP4 ablation leads to severely impaired fertility. *Figure 2 continued on next page*

Figure 2 continued

not affect ovulation (B), cleavage (C) and blastocyst (D) rates, preantral (E) and antral (F) follicles counts or pronuclei formation rate (G). The number of females (A–B), embryos (C–D and G) and slides (E–F) analysed per group is indicated inside each column. Data are represented as mean \pm SEM in all graphs. Statistical differences are based on ANOVA ($p < 0.05$, (A–D) or t-test ($p < 0.05$, (E–F). (H) Representative images of zygotes obtained from WT or KO females showing normal pronuclear formation (SYTOX green staining) in the presence (WT) or absence (KO) of ZP4 in ZP.

DOI: <https://doi.org/10.7554/eLife.48904.005>

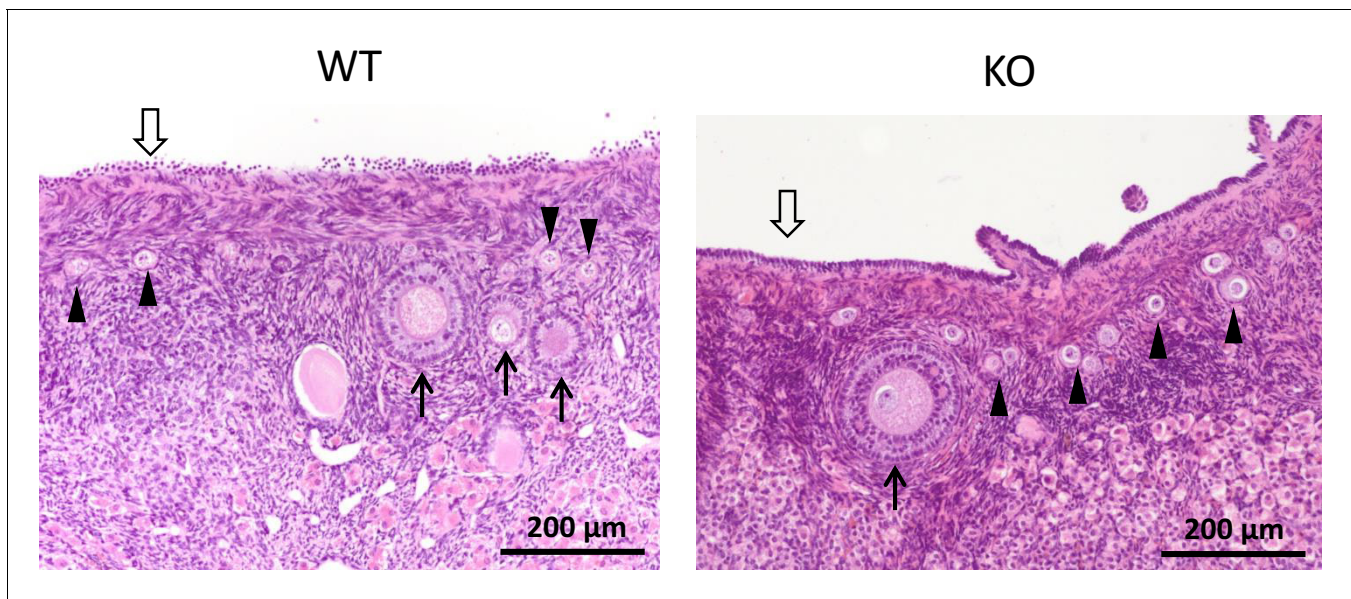


Figure 2—figure supplement 1. ZP4 ablation does not cause significant alterations in folliculogenesis. Histological sections of WT and ZP4 KO ovaries stained with haematoxylin-eosin, showing an overtly normal histological structure of ZP4 KO ovaries. Arrowheads point primordial follicles, solid arrows ovarian follicles and empty arrow the germinal epithelium.

DOI: <https://doi.org/10.7554/eLife.48904.006>

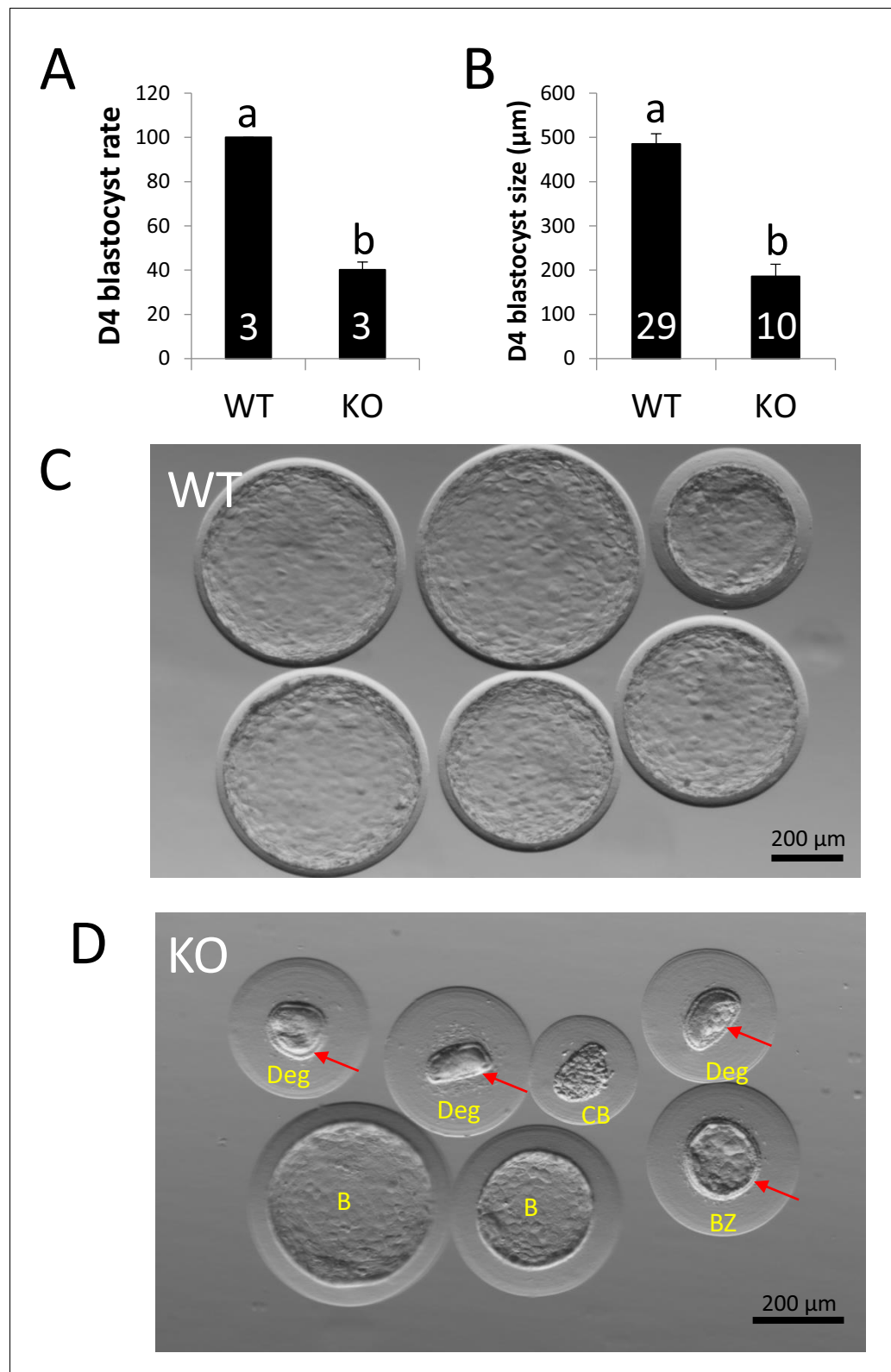


Figure 3. ZP4 ablation impairs blastocyst development in vivo. (A) Percentage of recovered embryos that had developed to the blastocyst stage by Day 4 post-mating. (B) Diameter (μm) of the blastocysts recovered on Day 4. The number of females (A) or blastocysts (B) analysed per group is indicated inside each column. In both graphs data are represented as mean \pm SEM and statistical differences are based on t-test ($p < 0.05$). (C) Representative Figure 3 continued on next page

Figure 3 continued

picture of Day four embryos obtained from WT females. (D) Representative picture of Day 4 embryos obtained from KO females. Red arrows indicate the presence of zona pellucida in some of the structures recovered and yellow letters indicate different types of structures found: Two expanded –yet smaller than those from WT females– blastocysts without zona (B), a collapsed blastocysts (CB) where zona was dissolved displaying a crunched appearance, a smaller expanded blastocyst retaining zona and showing also some degree of mechanical deformation (BZ), and three degenerated embryos (Deg) showing crunched zonae likely due to mechanical damage. Blastomeres (indicating several rounds of cell division before developmental arrest prior to compactation) can be easily spotted on the degenerated embryo on right.

DOI: <https://doi.org/10.7554/eLife.48904.007>

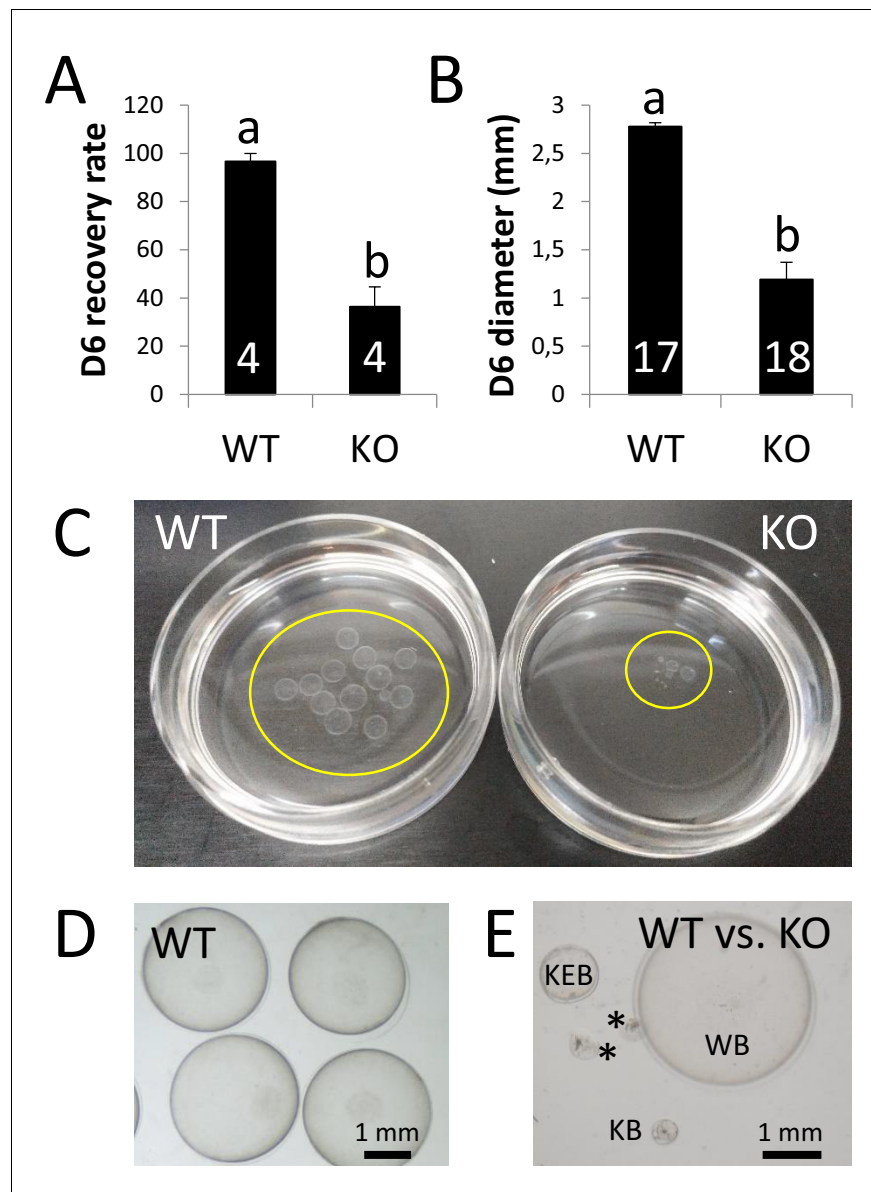


Figure 4. ZP4 ablation leads to severely impaired in vivo development to expanded blastocyst. (A) Recovery rate (embryos recovered/corpora lutea) on Day 6 was significantly reduced in KO females compared with WT counterparts. (B) Embryo diameter by Day 6 of in vivo development was significantly inferior in the few embryos recovered from KO females compared to WT counterparts. The number of females (A) or blastocysts (B) analysed per group is indicated inside each column. In both graphs data are represented as mean \pm SEM and statistical differences are based on t-test ($p < 0.05$). (C) Representative picture of Day 6 embryos recovered from a WT (left) or KO (right) female. Embryos were placed on 35 mm dishes. Yellow circles mark the location of the embryos inside the dishes. (D–E) Representative pictures of Day 6 embryos recovered from WT (D) or WT and KO (E) females. (E) 'WB' is a Day 6 blastocyst from the WT group, whereas the other structures were recovered from a KO female: KEB is an expanded blastocyst, KB a blastocyst showing a lesser degree of expansion and asterisks mark two degenerated embryos.

DOI: <https://doi.org/10.7554/eLife.48904.008>

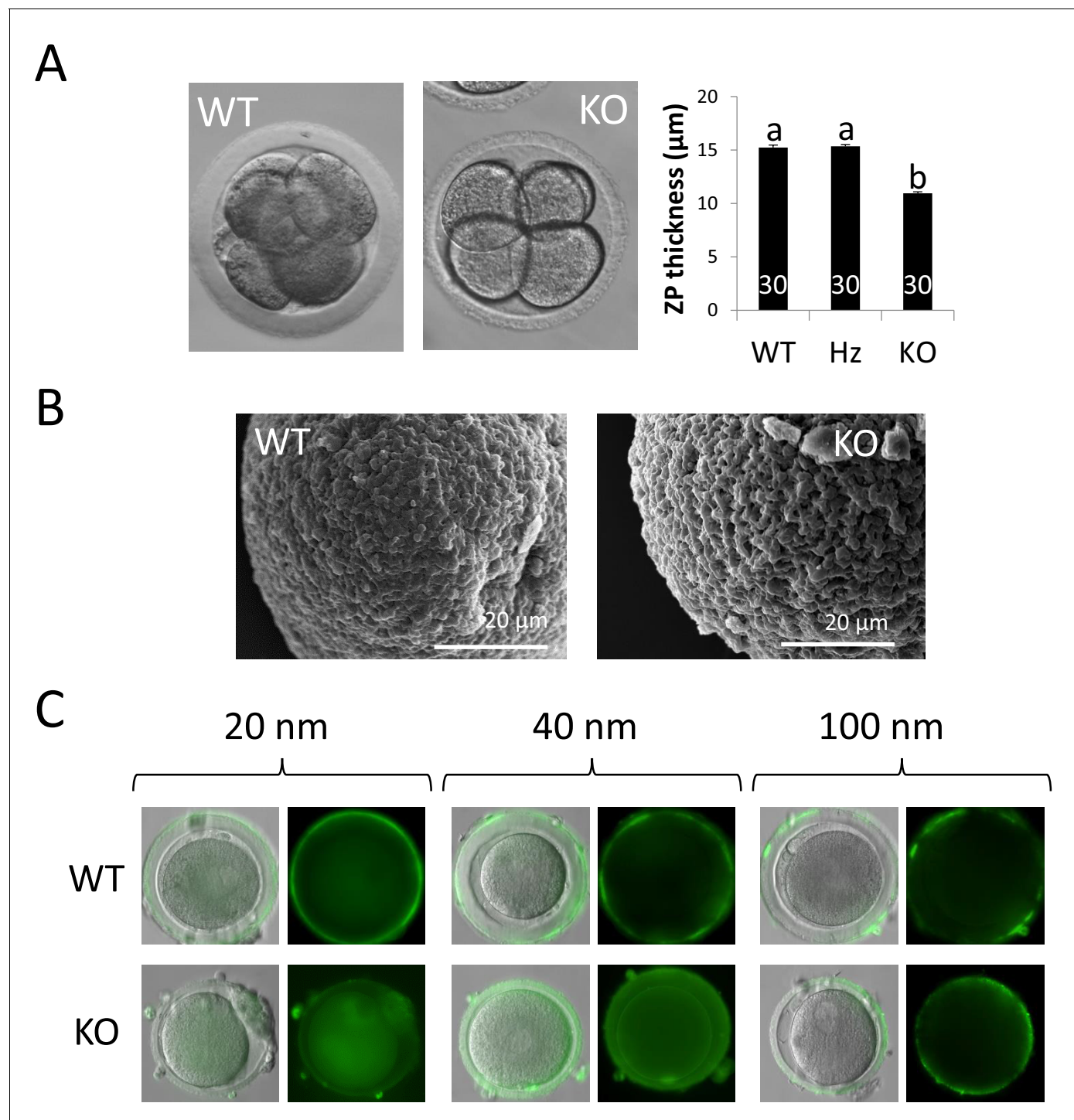


Figure 5. ZP4-devoided zona show structural abnormalities. (A) Representative pictures of cleaved embryos enclosed in ZP with (left) or without (right) ZP4 protein. ZP lacking ZP4 was significantly thinner than WT ZP. Hz females produced ZP overtly undistinguishable from WT counterparts. Data are represented as mean \pm SEM and statistical differences are based on ANOVA ($p < 0.05$). (B) Surface Electron Microscopy (SEM) pictures of ZP with (left) or without (right) ZP4 protein. In the absence of ZP4, ZP texture looks rougher and more fenestrated. (C) Fluorescent nanospheres permeability test in zygotes surrounded by ZP with (upper row) or without (lower row) ZP4 protein. WT and KO ZP blocked 100 nm particles, as fluorescence was restricted to the outer surface of ZP in both groups (right images). In contrast, all 9 ZP4-devoided ZP analyzed were permeable to 20–40 nm nanospheres, as green fluorescence inside ZP was evident (left and central images). No green fluorescence can be observed inside WT ZP, indicating that 20–40 nm nanospheres were efficiently blocked by a ZP containing ZP4. Statistical differences based on Chi-square test ($p < 0.05$).

DOI: <https://doi.org/10.7554/eLife.48904.009>

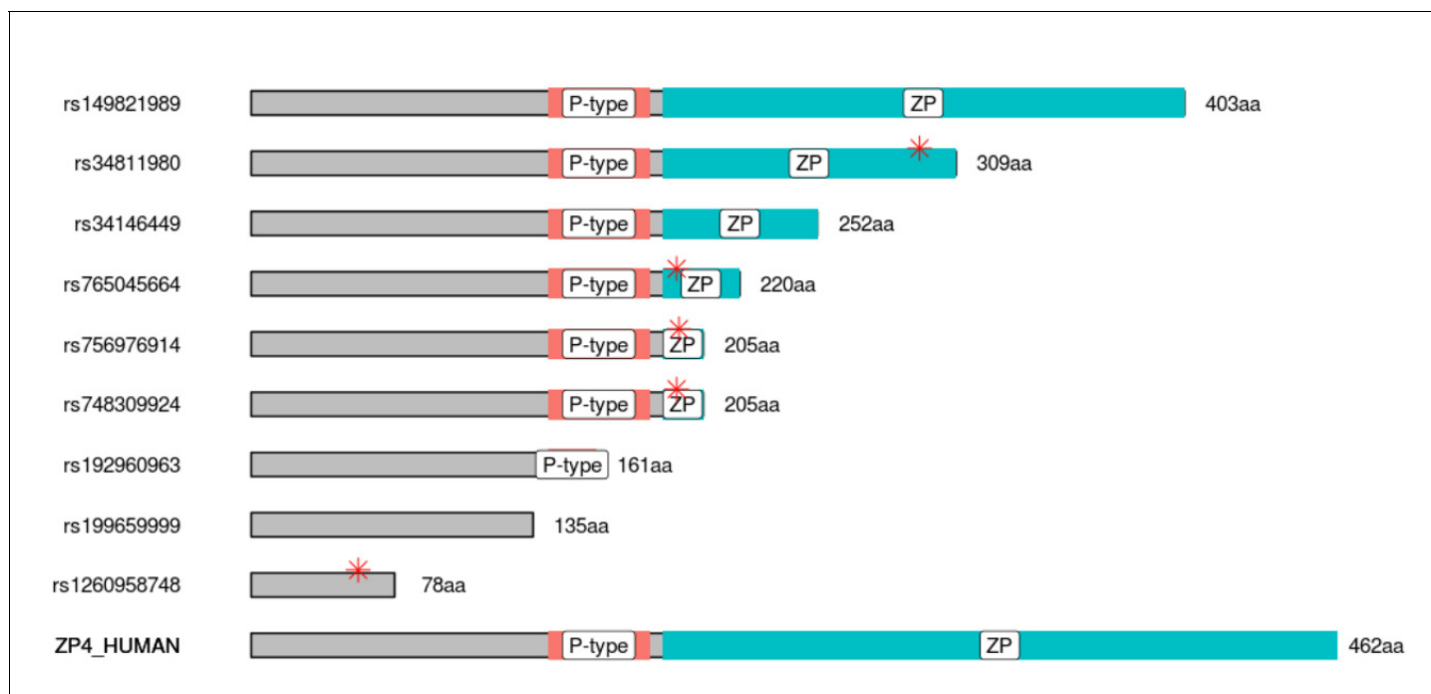


Figure 6. Polymorphism leading to truncated human ZP4 protein can be found at gnomAD database. Graphical representation of the human truncated proteins generated by the nine most frequent premature stop codon (PTCs) polymorphisms found in gnomAD database. Orange bars depicts P-type (trefoil domain), blue bars correspond to ZP domain, and red asterisks mark the position of the first amino acid affected by frame shift mutation (i.e., the end of the WT protein sequence).

DOI: <https://doi.org/10.7554/eLife.48904.011>